Experimental and numerical study of low impact damage in composite materials

Zheng He, Xuan Gu [a,*], Xiaoyu Sun, Jianxin Teng, YingShu Pang

College of Aerospace and Civil Engineering, Harbin Engineering University, Harbin 150001 China

[a]guxuan@hrbeu.edu.cn

Abstract

An experimental and numerical study on the influence of biaxial preloading on the low velocity impact performance of E-glass/epoxy-laminated composite plates was conducted. For this aim, an experimental device was developed to apply the load in two perpendicular directions. Three preload cases, representative of actual structures were selected, biaxially tension, compression and, tension-compression (shear) loading cases. The samples were produced from unidirectional reinforced E-glass and epoxy, by using a hand lay-up technique. Laminated E-glass/epoxy with stacking sequence [0/90]2s, dimensions were 140 × 140 mm2 and a thickness of 2 mm for the samples used. Finite element analysis (FEA) was developed, using Hashin failure criteria for the composite material, and material models implemented by a User Material Subroutine into ABAQUS®/explicit software, in order to simulate the failure mechanisms and force–time histories. Force–time and energy–time data were obtained by means of user material subroutine from the finite element model. The finite element results showed a good correlation to the experimental data in terms of force–time, energy–time graph or failure in composite plate, although these numerical results strongly depended on simulation parameters like mesh size or the number of element.

Keywords

Preloading; Composite plate; Low velocity impact; Finite element analysis.

1. Introduction

Recently, numerous researchers have been studying the impact response of laminated composites. Most of these researchers focus on laminated composites that are unloaded before low velocity impact[1-5]. But with regard to applications industry, it is rather unlikely that the impacted structures are unloaded. The composite structure may be subject to tensile, compressive or shear loads during their life-time of service. Therefore, it is necessary to determine the effect of preloading on the impact response of composite laminates. In the literature, there is a scarcity of information on the effect of preloading on the impact response of composite laminates.

A relatively small number of researchers have analyzed the behavior of preloaded structures subjected to low-velocity impact, the researchers studied experimental[6-11], numerical[12-14] both experimental and numerical[15-17] which discuss the impact response of different composite laminates. Some of these researchers focus on plates forced uniaxial or biaxial in-plane load, uniaxial tensile[7-9], biaxial tensile [11], uniaxial tensile and biaxial tensile–compressive (shear) [10] subjected to low velocity impacts.

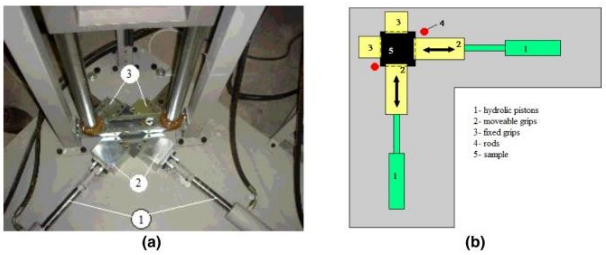

Fig. 1. (a) Preloading system; 1-hydrolic pistons, 2-moveable grips, 3-fixed grips and (b) schematic drawing.

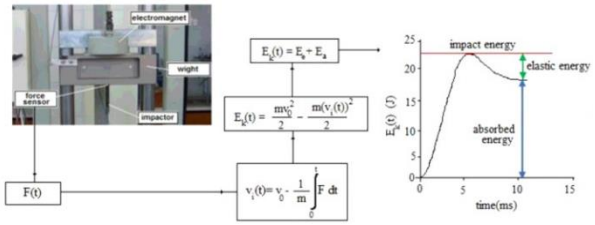

Fig. 2. Impact energy level, absorbed energy, and elastic energy [6].

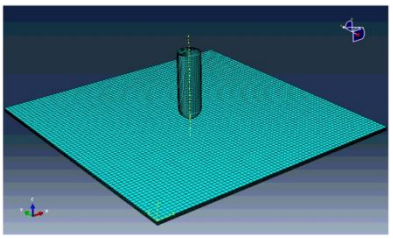

Fig. 3. A three dimensional finite element model for low velocity impact simulations on preloaded composite plate.

2. Materials And Methods

The samples were manufactured from unidirectional reinforced E-glass and epoxy at Izoreel Firm, by using a hand lay-up technique. Laminated E-glass/epoxy with stacking sequence [0/90]2s, the dimensions were 140 × 140 mm2 with a thickness of 2 mm for the samples used. In order to determine the mechanical properties of the composite laminate, several static tests were performed with respect to the standards of ASTM D3039-76 (ASTM D 3039-76, 1990) – ASTM D3410 (ASTM D 3410-87, 1990) – ASTM D3846-79 (ASTM D 3846-79, 1990). These material properties were used in the finite element simulations.

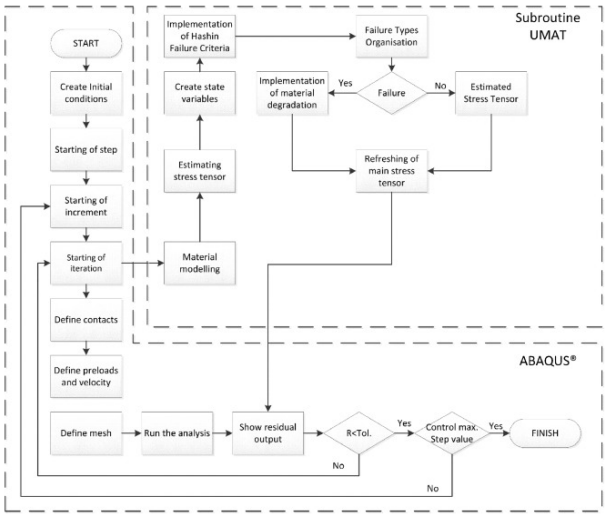

Fig. 4.Flow chart of the UMAT subroutine and ABAQUS®software.

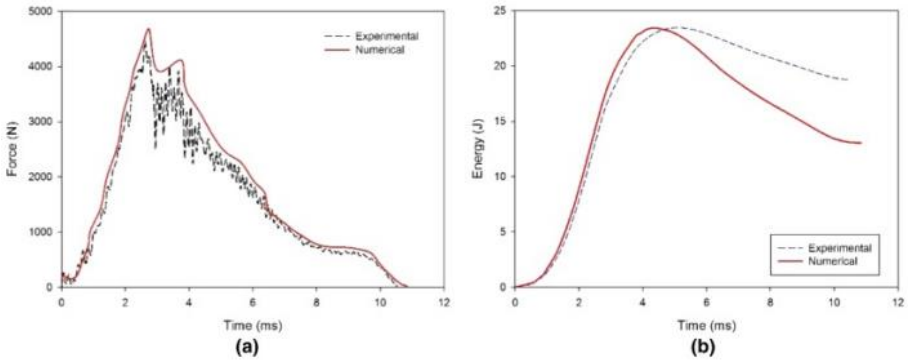

Fig. 5. Experimental and numerical impact results for non-preloading condition, (a) force–time histories and (b) energy–time histories.

In this study, a semi-spherical impactor with a 12 mm diameter was used. Impacts were applied in the middle points of the specimens and specimens were preloaded from four sides before impact. Three preload cases representative of actual structures were selected; biaxially tension, compression, and tension–compression (shear) loading cases. For preloading, four grips mounted on the base plate were used to restrain the test specimen. Two grips are moveable and the other two are fixed. Preloads could be given in tension–tension, compression–compression, and tension–compression (shear) in a biaxial way (Fig. 1). The control unit which is located near the testing device is used to control the hydraulic pistons.

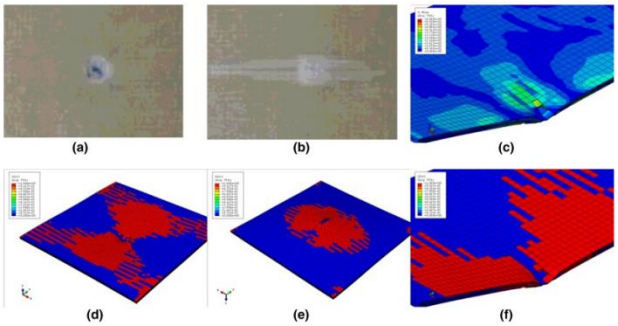

Fig. 6.Experimental and numerical failure mechanisms and stress distribution for non-preloading condition, (a) experimental front side, (b) experimental back side, (c) FEM stress distribution for cross section, (d) total Hashin failure front, (e) total Hashin failure back, and (f) total Hashin failure for cross section.

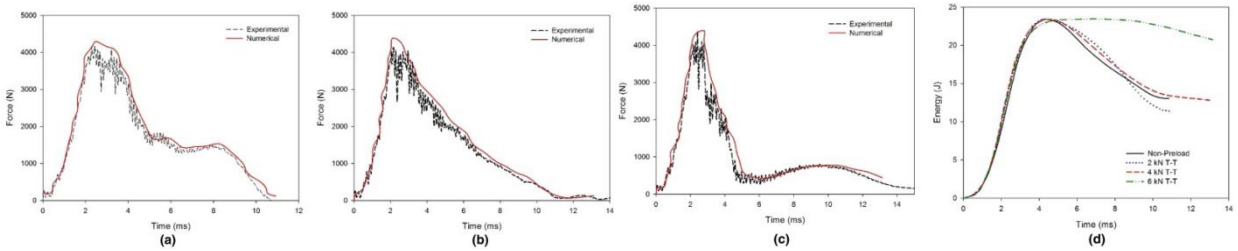

Fig. 7. Experimental and numerical impact results for biaxial tension preloading condition, (a) 2k N preload, (b) 4 kN preload, (c) 6 kN preload and (d) Numerical energy–time histories for biaxial tension preloading and non-preloading conditions.

3. Results And Discussion

Fig. 5a gives the force–time histories of the center node of the plate and compares the results from all the experimental results from Kurşun and Şenel [6] with the results from this study for non-preloading condition. In general, the contact force level increases rapidly at the beginning, which is the result of an oscillation of the composite plate after first contact with the impactor. When the plate reaches maximum deflection, the force level decreases to zero again. Fig. 5b shows experimental energy–time histories which were calculated from the force–time histories, but numerical results were directly

obtained from the FE model. The energy versus time increases continuously and reaches to a level of impact energy, and then fall to a certain level. The impact energy level minus certain level value is an indicator for the absorbed energy, which is not transferred to the impactor as elastic spring back. If the plate behaved completely elastic without failure and neglect of friction losses, the energy curve would return to zero again. As it can be seen from these figures, the finite element results showed a good correlation to the experimental data in terms of force–time and energy–time graphs.

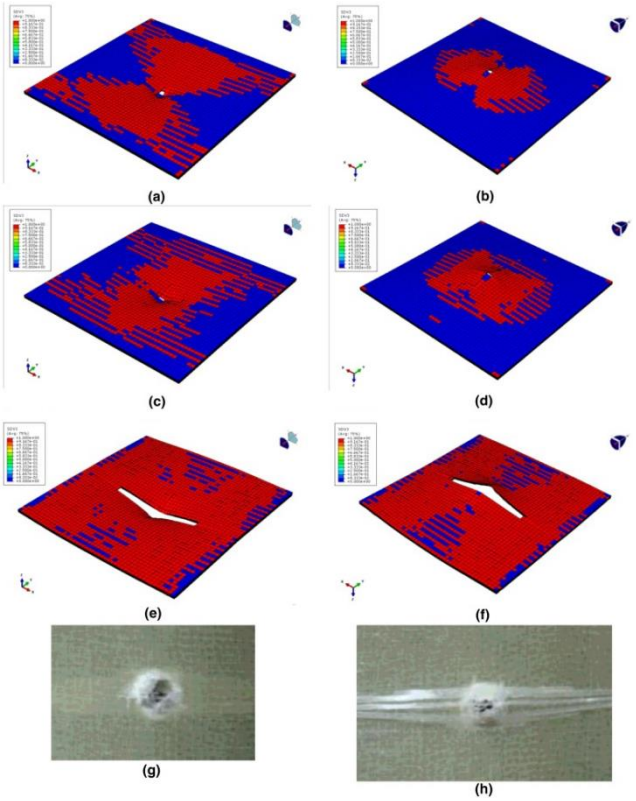

Fig. 8. Total Hashin failure results for biaxial tension preloading condition, (a) 2 kN front, (b) 2 kN back, (c) 4 kN front, (d) 4 kN back, (e) 6 kN front, (f) 6 kN back, (g) 6 kN front experimental and (h) 6 kN back experimental.

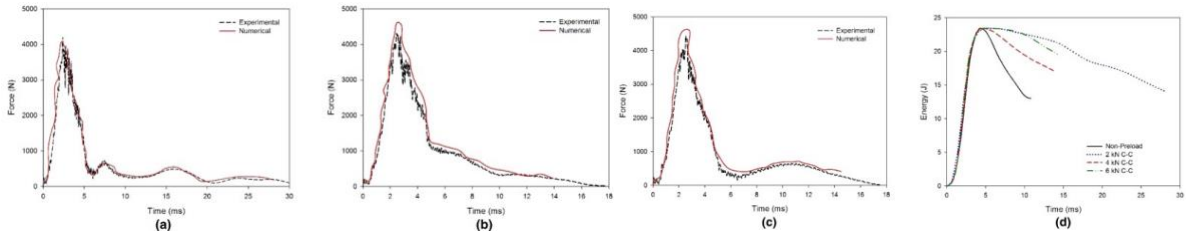

Fig. 9. Experimental and numerical impact results for biaxial compression preloading condition, (a) 2 kN preload, (b) 4 kN preload, (c) 6 kN preload and (d) numerical energy–time histories for biaxial compression preloading and non-preloading conditions.

Fig. 7(a–(c) illustrates force–time histories for 2 kN, 4 kN, 6 kN biaxial tensions, respectively. As seen in these figures, the contact force takes maximum value (*F*exp = 4387, 33 N and*F*num = 4396, 65 N) for 6 kN biaxial tension preloading and minimum (*F*exp = 4164, 97 N and*F*num = 4295, 37 N) for 2 kN biaxial tension preloading. The contact time is the highest for 6 kN biaxial tension preloading. Also, it was observed that the contact force and time increased with the increase of the biaxial tension preloading. The biaxial tension preloading induces a stiffening effect on the sample which would explain the higher contact force. However, the contact forces both numerical and experimental take maximum value for non-preloading condition. Comparing with the results of biaxial tension preloading and non-preloading condition, it can be said that the impact damages occur faster with the increase of the biaxial tension preloading.

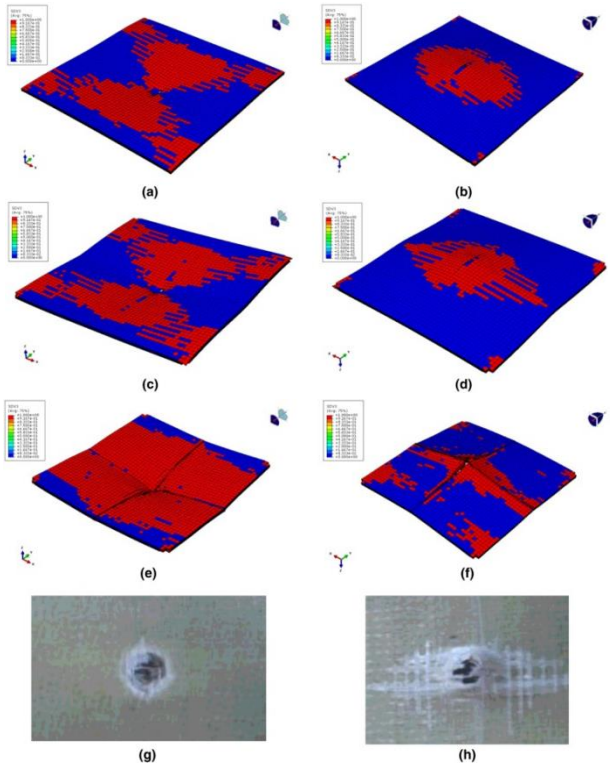

Fig. 10. Total Hashin failure results for biaxial compression preloading condition, (a) 2 kN front, (b) 2 kN back, (c) 4 kN front, (d) 4 kN back, (e) 6 kN front, (f) 6 kN back, (g) 6 kN front experimental and (h) 6 kN back experimental.

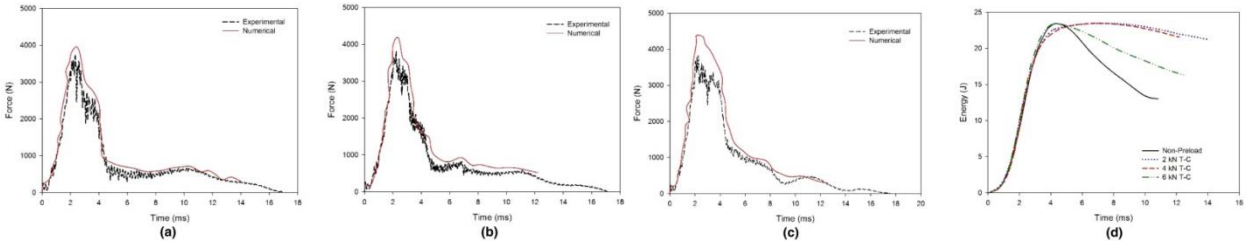

Fig. 11. Experimental and numerical impact results for tension–compression (shear) preloading condition, (a) 2 kN preload, (b) 4 kN preload, (c) 6 kN preload and (d) numerical energy–time histories for tension–compression (shear) preloading and non-preloading conditions.

Energy–time histories of the preloading and non-preloading conditions on composite plates are shown in Fig. 7(d). Given the comparisons with respect to energy–time histories, the absorbed energy values increase with the preloading increase, and the highest absorbed energy is obtained in the specimen in which for 6 kN biaxial tensions preloading is applied.

It is seen that for all the cases (a– (h) considered in Fig. 8, the damages occur at the center of the plate and they are expanded around the center. It can be observed that the Hashin failure increased with the increase of the biaxial tension preloading. However, FE results for low velocity impact on preloaded composite plate, such as damage zone and shape, showed a poor correlation with the experimental results (Fig.8e–h), when the biaxial tension preloading increases.

The results for the biaxial compression preloading cases are shown in Fig. 9. The correlation between the experimental and FEM results are acceptable. As seen in these figures, the contact force takes maximum value (*F*exp = 4431, 85 N and *F*num = 4571, 96 N) for 6 kN biaxial compression preloading and minimum (*F*exp = 4197, 05 N and *F*num = 4072, 48 N) for 2 kN biaxial compression preloading.

Energy–time histories of the biaxial compression preloading and non-preloading conditions on composite plates are shown in Fig. 9(d). Given the comparisons with respect to energy–time histories, the absorbed energy values increased with the preloading increase and the highest absorbed energy is obtained in the specimen, in which for 6 kN biaxial compression preloading is applied. FE results

for various biaxial compression preloads are shown in Fig. 10, the damages occur at the center of the plate and they are expanded around the center. It can be observed that the FE predictions for low velocity impact on preloaded composite plate, such as damage zone and shape, showed a poor correlation with experimental results (Fig. 10e–h), when the biaxial compression preloading increased.

Effects of the tension–compression (shear) preloading on time histories of the contact force and energy are illustrated in Fig. 11. As seen in these figures, the contact force takes maximum value (*F*exp = 3826, 18 N and *F*num = 4381, 61 N) for 6 kN shear preloading and minimum (*F*exp = 3722, 19 N and *F*num = 3956, 33 N) for 2 kN shear preloading. However, the contact force both numerical and experimental takes maximum value for non-preloading condition.

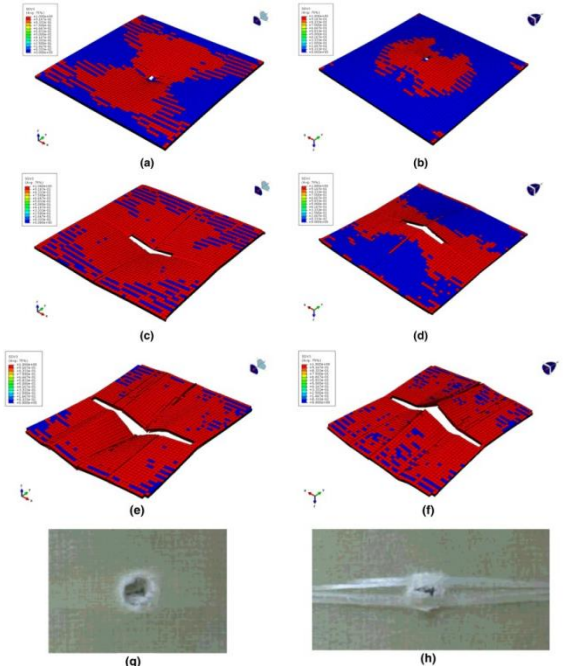

Fig. 12. Total Hashin failure results for tension–compression (shear) preloading condition, (a) 2 kN front, (b) 2 kN back, (c) 4 kN front, (d) 4 kN back, (e) 6 kN front, (f) 6 kN back, (g) 6 kN front experimental and (h) 6 kN back experimental.

Energy–time histories of the tension–compression (shear) preloading and non-preloading conditions on composite plates are shown in Fig. 11(d). The absorbed energy takes maximum value (*E*abs = 21, 49 J experimental and *E*abs = 16, 21 J Numerical) for 6 kN shear preloading and minimum (*E*abs = 18,74 J experimental and *E*abs = 13,03 J Numerical) for non-preloading conditions. Therefore, composite material damage increases with the increase of the tension–compression preloading.

FE predictions of total Hashin failure for various shear preloads are shown in Fig. 12. It can be observed that the FE predictions for low velocity impact on preloaded composite plate, such as damage zone and shape, showed a poor correlation with the experimental results (Fig. 12 e– h), when the biaxial preloading increases.

4. Conclution

In this study, a numerical study on the influence of an in-plane biaxial load on the impact behaviour of E-glass/epoxy-laminated composites plates was analyzed. Finite element analysis (FEA) was developed, using Hashin failure criteria for the composite material and material models implemented by User Material Subroutine into ABAQUS® software, in order to simulate the failure mechanisms, force and energy–time histories. Some general observations of this study can be summarized as follows:

It can be concluded from the experimental and numerical results, the rigidity of the material increased with the effect of preloading. Therefore, damage in relation to the specimens increased as the elastic capability of the material decreases.

The experimental and FEM results showed an increased deflection for the preloaded composite plates, which lead to a higher extent of material damage compared to the unloaded plates.

The experimental and FEM results showed an increased absorbed energy for the preloaded composite plates. Therefore, composite material damage was higher compared to the unloaded plates.

The contact force and time are increased with the increase of the biaxial tension preloading.

The biaxial preloading induces a stiffening effect on the sample which results in the higher contact force.

The FE results showed a good correlation to the experimental data in terms of force and energy–time histories.

FE results, such as damage zone and shape showed a poor correlation with the experimental results when the biaxial preloading increased.

Acknowledgements

This work is supported by the National Natural Science Foundation of China（No. 11602066） and the National Science Foundation of Heilongjiang Province of China (QC2015058 and 42400621-1-15047), the Fundamental Research Funds for the Central Universities.

References

[1] I. Taraghi, A. Fereidoon, F. Taheri-Behrooz Low-velocity impact response of woven Kevlar/epoxy laminated composites reinforced with multi-walled carbon nanotubes at ambient and low temperatures Mater Des, 53 (2014), pp. 152–158

[2] Z. Aslan, R. Karakuzu, B. Okutan The response of laminated composite plates under low-velocity impact loading Compos Struct, 59 (2003), pp. 119–127

[3] G. Minak, D. Ghelli Influence of diameter and boundary conditions on low velocity impact response of CFRP circular laminated plates Compos Part B: Eng, 39 (2008), pp. 962–972

[4] F. Mili, B. Necib Impact behavior of cross ply laminated composite plates under low velocities composite-structures Compos Struct, 51 (2001), pp. 237–244

[5] S. Xiao, P. Chen, Q. Ye Prediction of damage area in laminated composite plates subjected to low velocity impact Compos Sci Technol, 98 (2014), pp. 51–56

[6] A. Kursun, M. Senel Investigation of the effect of low-velocity impact on composite plates with preloading Exp Tech, 37 (2013), pp. 41–48

[7] N. Guillaud, C. Froustey, F. Dau, P. Viot Impact response of thick composite plates under uniaxial tensile preloading Compos Struct, 121 (2015), pp. 172–181

[8] H. Saghafi, G. Minak, A. Zucchelli Effect of preload on the impact response of curved composite panels Compos Part B: Eng, 60 (2014), pp. 74–81

[9] H. Saghafi, T. Brugo, G. Minak, A. Zucchelli The effect of pre-stress on impact response of concave and convex composite laminates Procedia Eng, 88 (2014), pp. 109–116

[10] B. Whittingham, I.H. Marshall, T. Mitrevski, R. Jones The response of composite structures with pre-stress subject to low velocity impact damage Compos Struct, 66 (2004), pp. 685–698

[11] T. Mitrevski, I.H. Marshall, R.S. Thomson, R. Jones Low-velocity impacts on preloaded GFRP specimens with various impactor shapes Compos Struct, 76 (2006), pp. 209–217

[12] M.H. Malik, Arif AFM ANN prediction model for composite plates against low velocity impact loads using finite element analysis Compos Struct, 101 (2013), pp. 290–300

[13] M. Shariyat, S.H. Hosseini Accurate eccentric impact analysis of the preloaded SMA composite plates, based on a novel mixed-order hyperbolic global–local theory Compos Struct, 124 (2015), pp. 140–151

[14] K.M. Mikkor, R.S. Thomson, I. Herszberg, T. Weller, A.P. Mouritz Finite element modelling of impact on preloaded composite panels Compos Struct, 75 (2006), pp. 501–513

[15] M.A. Hassan, S. Naderi, A.R. Bushroa Low-velocity impact damage of woven fabric composites: finite element simulation and experimental verification Mater Des, 53 (2014), pp. 706–718

[16] S. Heimbs, S. Heller, P. Middendorf, F. Hähnel, J. Weiße Low velocity impact on CFRP plates with compressive preload: test and modelling Int J Impact Eng, 36 (2009), pp. 1182–1193
[17] V. Tita, J. de Carvalho, D. Vandepitte Failure analysis of low velocity impact on thin composite laminates: experimental and numerical approaches Compos Struct, 83 (2008), pp. 413–428